



Enhanced ultraviolet emission and its irreversible temperature antinquenching behavior of twofold coordinated silicon centers in silica glass

Nagayoshi, Yu
Uchino, Takashi

(Citation)

Applied Physics Letters, 109(18):181103-181103

(Issue Date)

2016-10-31

(Resource Type)

journal article

(Version)

Version of Record

(Rights)

©2016 AIP Publishing. This article may be downloaded for personal use only. Any other use requires prior permission of the author and AIP Publishing. The following article appeared in Applied Physics Letters 109(18), 181103 and may be found at <http://dx.doi.org/10.1063/1.4966952>

(URL)

<https://hdl.handle.net/20.500.14094/90003742>



Enhanced ultraviolet emission and its irreversible temperature anti-quenching behavior of twofold coordinated silicon centers in silica glass

Yu Nagayoshi and Takashi Uchino

Citation: *Appl. Phys. Lett.* **109**, 181103 (2016); doi: 10.1063/1.4966952

View online: <http://dx.doi.org/10.1063/1.4966952>

View Table of Contents: <http://aip.scitation.org/toc/apl/109/18>

Published by the [American Institute of Physics](#)

Articles you may be interested in

[Time-resolved photoluminescence characterization of oxygen-related defect centers in AlN](#)

Applied Physics Letters **109**, 021113 (2016); 10.1063/1.4958891

AIP | Applied Physics
Letters

Save your money for your research.
It's now **FREE** to publish with us -
no page, color or publication charges apply.

If your article has the
potential to shape the future of
applied physics, it BELONGS in
Applied Physics Letters

Enhanced ultraviolet emission and its irreversible temperature anti-quenching behavior of twofold coordinated silicon centers in silica glass

Yu Nagayoshi and Takashi Uchino^{a)}

Department of Chemistry, Graduate School of Science, Kobe University, Nada, Kobe 657-8501, Japan

(Received 28 July 2016; accepted 21 October 2016; published online 1 November 2016)

It has been well documented that an oxygen divacancy center, or a twofold-coordinated Si center, in silica glass yields a singlet-to-singlet photoluminescence (PL) emission at 4.4 eV with a decay time of ~ 4 ns. Although the 4.4-eV PL band is interesting in terms of a deep-ultraviolet light emitter, the emission efficiency has been too low to be considered for a practical application. In this work, we show that a highly luminescent silica glass, with an internal quantum yield of 68% for the 4.4-eV PL band at room temperature, can be prepared when micrometer-sized silica powders are heat treated at $\sim 1900^\circ\text{C}$ under inert gas atmosphere by using a high-frequency induction heating unit equipped with a graphite crucible. We also show that the intensity of the 4.4-eV emission in the thus prepared silica glass exhibits an irreversible temperature anti-quenching behavior in the temperature region below ~ 320 K during heating-cooling cycles. The anomalous temperature dependencies of the 4.4-eV emission can be interpreted in terms of thermally activated trapping-detrapping processes of photoexcited electrons associated with deep trap states.

Published by AIP Publishing. [<http://dx.doi.org/10.1063/1.4966952>]

Amorphous silica (or glassy silica, g-SiO₂) is one of the most extensively studied oxides in condensed matter physics, materials science, and related engineering fields.^{1,2} This is because it not only provides a model for disordered amorphous systems,^{3–5} but it also finds widespread industrial applications ranging from electronic devices⁶ to state-of-the-art optical communication systems.^{7,8} It has been recognized that electrical, optical, and mechanical properties of g-SiO₂ are governed by the quantity and quality of intrinsic and/or extrinsic defects introduced during the fabrication process. Thus, the structure and properties of defect centers in g-SiO₂ have been investigated previously by many researchers both by theoretical and experimental means.^{9–12}

Among other defect related properties in g-SiO₂, the optical absorption at ~ 5 eV and the related photoluminescence (PL) at 4.4 and 2.8 eV have been extensively studied during the past decades.^{13–19} Although several models have been proposed previously, it is now commonly accepted that twofold-coordinated Si centers are responsible for these absorption and emission bands.^{20–23} According to Skuja,^{16,20} the basic optical properties of the twofold-coordinated defect centers can be explained by the simplified energy level scheme of a singlet ground state (S_0) and excited triplet (T_1) and singlet (S_1) states. That is, the twofold-coordinated Si gives rise to the singlet absorption band ($S_0 \rightarrow S_1$) at ~ 5 eV and the singlet ($S_1 \rightarrow S_0$) and triplet ($T_1 \rightarrow S_0$) luminescence bands at 4.4 and 2.8 eV, respectively. In view of applications, the $S_1 \rightarrow S_0$ emission at 4.4 eV, which is the dominant emission component at room temperature, would be of potential interest in producing deep-ultraviolet (UV) emitting materials. However, the efficiency of the $S_1 \rightarrow S_0$ emission at 4.4 eV

is generally too low at room temperature to be seriously considered for practical applications.

To overcome these problems, we propose here a method to increase the emission efficiency of two-fold coordinated Si centers in g-SiO₂. We have previously demonstrated that the high-frequency induction heating, when combined with a graphite crucible, is useful to introduce a large amount of oxygen vacancies in refractory oxides such as sapphire ($\alpha\text{-Al}_2\text{O}_3$)^{24,25} and magnesium aluminate spinel (MgAl_2O_4).²⁶ The graphite crucible is used not only as an electrically conductive object for induction heating but also as a reducing agent. Thus, it is expected that this induction heating method is effective in introducing oxygen vacancies, including twofold-coordinated Si, in g-SiO₂ as well. In this work, we show that the emission quantum efficiency of the 4.4-eV band can be raised to $\sim 70\%$ when silica powders are heat-treated under inert atmosphere at $\sim 1900^\circ\text{C}$ by the high-frequency induction heating method. We also demonstrate that the present sample exhibits an irreversible temperature anti-quenching behavior of the 4.4-eV PL band. Such hysteretic temperature dependence is interpreted in terms of the thermally activated trapping/detrapping processes of photoexcited electrons in some deep traps.

We used high-purity g-SiO₂ powders (purity 99.999% and average particle size $63\ \mu\text{m}$, Kojundo Chemical Laboratory Co., LTD) as starting materials. We heated the g-SiO₂ powders (~ 0.2 g) under a flowing inert gas (N₂ or Ar) atmosphere in a graphite crucible by using a high-frequency induction heating unit, which is rated at 4 kW at a maximum frequency of 420 kHz. Heating under an inert atmosphere along with the use of a graphite crucible is the requisite to achieve highly reducing conditions during induction heating. The heating temperature was raised up to $\sim 1900^\circ\text{C}$ at a rate of $\sim 500^\circ\text{C}/\text{min}$ and maintained at the

^{a)} Author to whom correspondence should be addressed: Electronic mail: uchino@kobe-u.ac.jp

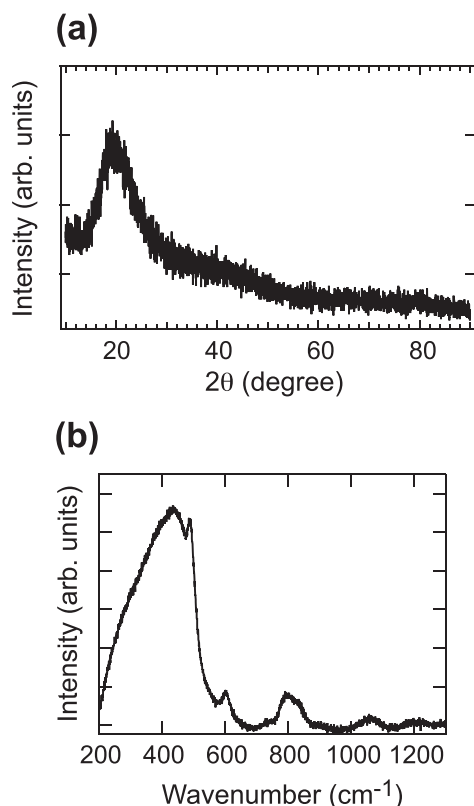


FIG. 1. (a) XRD pattern and (b) Raman spectrum of the induction-heated g-SiO₂.

same temperature for 2–3 min. The temperature of the system was monitored with a radiation thermometer. After the heating process, the system is naturally cooled to room temperature. As a result, a white opaque disk-shaped sample with a diameter of ~ 10 mm and a thickness of ~ 1 mm was obtained. We found that the structural and optical properties of the sample do not depend on the gas environment used for induction heating. Thus, in what follows, we will mainly show the results of the sample prepared under N₂ environment.

Powder X-ray diffraction (XRD) patterns of the ground sample were obtained with a diffractometer (Rigaku,

SmartLab) using Cu $K\alpha$ radiation. Raman spectra were measured with a Raman microscope (JASCO NRS-7100) at room temperature using a 532 nm line laser as an excitation source. Photoluminescence (PL) spectra were recorded on a spectrofluorometer (JASCO, FP 6600) with a monochromated xenon lamp (150 W). During the PL measurements, the sample temperature was controlled in a closed-cycle N₂ cryostat under a vacuum of 10 Pa in the temperature region from 78 to 500 K. The absolute PL quantum yield was obtained at room temperature with an integrated sphere system (Otsuka Electronics, QE-2000).

Figure 1 shows the XRD pattern and Raman spectrum of the g-SiO₂ sample after induction heating. The XRD pattern (Fig. 1(a)) shows a diffraction halo characteristic of glassy materials. Furthermore, the position and line shape of the Raman spectrum (Fig. 1(b)) are similar to those reported previously for g-SiO₂.^{27–29} Thus, we confirmed that the present sample is in the form of g-SiO₂ even after the induction heating process. We next investigate the PL properties of the sample. Although the as-received raw g-SiO₂ powders hardly show any emission under UV excitation, as shown in the inset of Fig. 2(a), the induction-heated g-SiO₂ sample exhibits an intense PL band at 4.4 eV, which is supposed to result from the S₁→S₀ emission of twofold-coordinated Si, under excitation with photons of 4.9 eV. To further characterize the 4.4-eV PL band of the induction-heated sample, the temperature dependent PL and PL excitation (PLE) spectra were measured on heating from 78 to 500 K (see Figs. 2(a) and 2(b)). One sees from Fig. 2(a) that in addition to the 4.4-eV PL band, the 2.8-eV PL band, which is attributed to the T₁→S₀ emission of twofold-coordinated Si,^{16,20} is developed in the temperature region above ~ 300 K under 4.9-eV excitation. It should be worth mentioning that the internal and external quantum yields of the 4.4 eV PL band are 68% and 55%, respectively, at room temperature. This suggests that a large amount of twofold-coordinated Si centers are introduced into the silica glass network during the induction heating process although its exact quantification is not possible at present.

To further explore the emission characteristics of the g-SiO₂ sample, the temperature dependence of the 4.4-eV

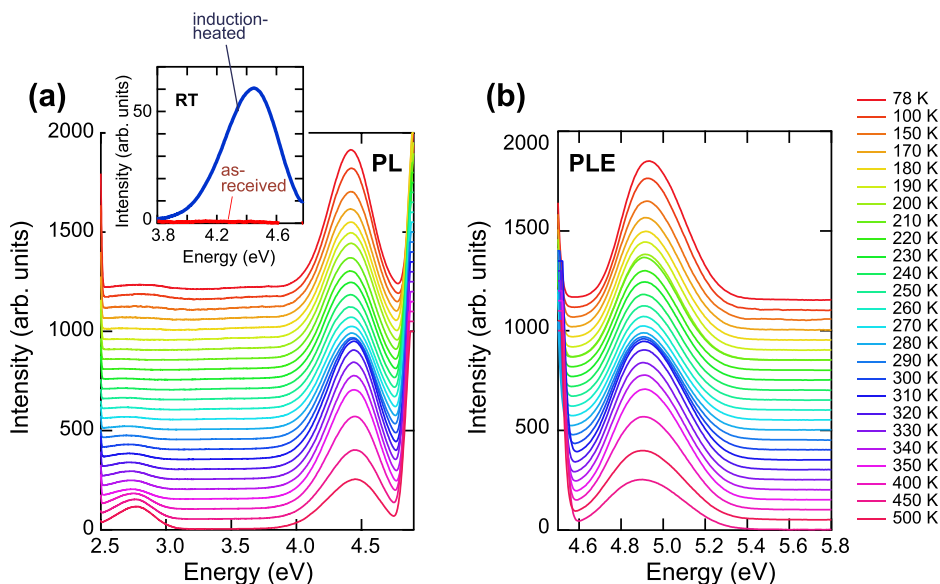


FIG. 2. (a) PL and (b) PLE spectra of the induction-heated g-SiO₂ measured on heating from 78 to 500 K. Before the measurements, the sample was cooled from room temperature to 78 K under dark condition. The excitation and monitoring energies are 4.9 and 4.4 eV, respectively. The inset in (a) shows the PL spectra of the as-received and the induction-heated g-SiO₂ measured at room temperature under 4.9-eV excitation.

PL band was measured in both the heating and cooling directions. For that purpose, we first cooled the sample down to 78 K in a dark environment and the PL spectra were measured on heating from 78 to 500 K. After the heating process, the sample was cooled from 500 to 78 K to measure the temperature dependent PL spectra during cooling. Figure 3(a) shows the peak intensity of the 4.4-eV PL band as a function of temperature measured in the heating and cooling directions.

To begin with, we analyze the change in the PL intensity with temperature during the heating process. As shown in Fig. 3(a), the 4.4-eV PL band shows a constant decrease in intensity with increasing temperature from 78 to ~ 250 K. As the temperature increases above 260 K, however, the PL intensity shows an increase and then reaches the maximum at a temperature of ~ 320 K. At temperatures above ~ 320 K, the PL intensity decreases once again. The observed irregular temperature dependence is different from that reported previously for the 4.4-eV PL band in g-SiO₂, where the peak intensity shows a monotonous decrease or a normal thermal quenching in a wide temperature region from ~ 100 to ~ 400 K.^{13,16,20,30}

Next, we investigate the temperature dependence in the cooling direction. Figure 3(a) shows that the PL response in the 320–500 K temperature range is quite reversible. In the cooling process, however, the PL intensity continues to rise with decreasing temperature down to ~ 280 K, followed by a slight decrease in intensity on further cooling (temperature anti-quenching). Thus, the present induction-heated sample exhibits an irreversible temperature anti-quenching behavior. When the temperature of the system goes below ~ 200 K, the PL intensity reaches an almost constant value. Note also that the PL intensity at 78 K obtained after the cooling process is lower than the starting value obtained initially at 78 K (see also the corresponding PL spectra shown in Fig. 3(b)). To confirm whether this difference results from the history of light irradiation, the sample was reheated up to 320 K, which is within the reversible temperature region, and was subsequently cooled to 78 K under dark condition; then we carried out the PL measurement at 78 K once again. We found that the resulting PL spectrum is almost identical to the initial PL spectrum observed at 78 K (see Fig. 3(b)), indicating that the previous irradiation history is erased when the temperature of the system is increased to 320 K.

It has been well recognized that multiphonon relaxation, in which the energy gap between the excited state and the

ground state is bridged by the simultaneous emission of phonons, is a major emission quenching process.³¹ This process is, in principle, reversible with temperature, and will not account for the irreversible PL behavior observed in this work. Another principal process for emission quenching results from thermally activated photoionization, which is induced by escape of a charge carrier from an emission center by thermally activated ionization.³¹ When the escaped charge carriers are captured by some deep traps, the related luminescence becomes weakened or quenched. Since the number of charge traps may depend on the previous thermal and irradiation history, the resulting PL signals could be irreversible with temperature,³² even leading to irreversible temperature anti-quenching, as observed in some core-shell quantum dots.³³

We hence consider that the irreversible temperature anti-quenching behavior observed in this work can also be interpreted in terms of the thermally activated trapping/detrapping processes associated with certain deep traps. A schematic representation of the energy levels for the ground and excited states of the twofold-coordinated Si and the related deep trap states is shown in Fig. 4(a). It would be reasonable to assume from Fig. 4(a) that the activation energy of photoionization (ΔE_1) is larger than that of detrapping (ΔE_2) from deep traps. Bearing this in mind, we depict in Fig. 4(b) a semi-quantitative description of the number of trapped electrons accumulated in the sample during the heating and cooling procedures.

When the sample is first cooled to 78 K under dark conditions, as in the case of the present experiments, the number of trapped electrons will be negligibly small (see point A in Fig. 4(b)). As the temperature of the system increases, the rate of thermally activated photoionization will increase, and, accordingly, an increasing number of escaped electrons are trapped and accumulated at deep trap states (see point B in Fig. 4(b)). This will (partly) account for the PL thermal quenching in the 78–250 K temperature range during heating shown in Fig. 3(a). At higher temperatures ($T \geq 260$ K), however, the trapped electrons will begin to be detrapped with the help of thermal energy (see points C, D in Fig. 4(b)) and will be returned to the emission center to eventually contribute to the 4.4-eV PL emission. The observed temperature anti-quenching in the 260–320 K range during heating can thus be explained in view of the thermally activated detrapping process. At temperatures higher than ~ 320 K, the number of trapped electrons will remain a constant low (near

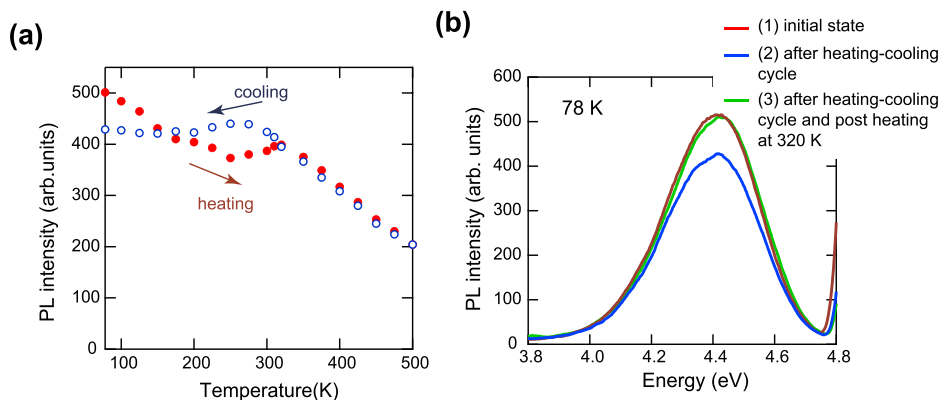


FIG. 3. (a) Temperature dependence of the peak intensity of the 4.4-eV PL band measured for the induction-heated g-SiO₂ during a heating-cooling cycle. Before carrying out the heating process, the sample was cooled from room temperature to 78 K under dark condition. (b) 78 K PL spectra for the sample with different thermal histories: (1) initial as-cooled state, (2) after the heating-cooling cycle, and (3) after the heating-cooling cycle and the subsequent post-heating at 320 K.

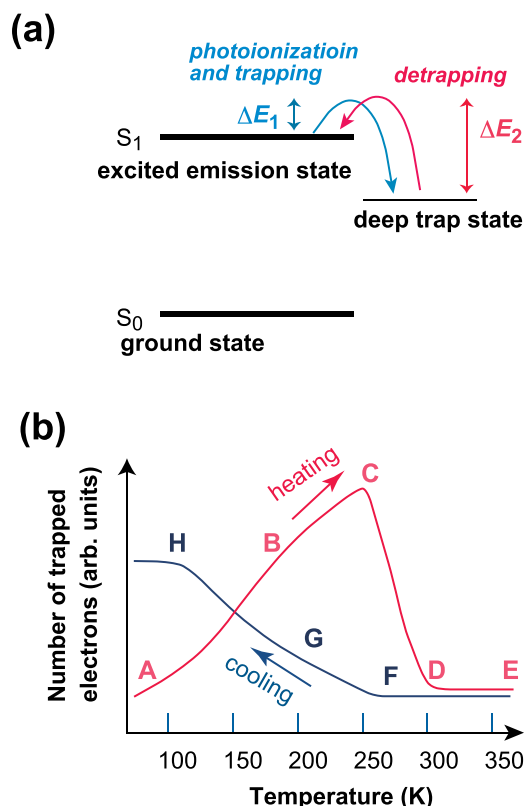


FIG. 4. (a) A schematic representation of the energy levels for the ground (S_0) and excited (S_1) states of the twofold-coordinated Si and the related deep trap states. (b) A semi-quantitative description of the number of trapped electrons accumulated in the sample during the heating-cooling cycle.

zero) value (see points D, E in Fig. 4(b)) because the rates of photoionization and detrapping events could become comparable at such high temperatures. As a result, multiphonon relaxation governs the entire nonradiative recombination process, explaining the reversible temperature quenching behavior in the ~ 320 to 500 K temperature range shown in Fig. 3(a).

According to the above scheme, it is natural to expect that the PL intensity measured on cooling just below ~ 320 K is higher than the corresponding PL intensity measured on heating. This is because in the temperature region just below ~ 320 K, the number of trapped electrons created during cooling will be much smaller than the one accumulated during heating (see point F in Fig. 4(b)). Upon further cooling, however, an appreciable amount of trapped electrons will be accumulated even on cooling (see point G in Fig. 4(b)) since the photoionization event with a lower activation energy begins to prevail over the detrapping event with a higher activation energy with decreasing temperature. This will lead to a temperature anti-quenching as in the case of the heating process although the temperature at which the PL intensity becomes maximum will be different between the cooling and heating directions, as observed in Fig. 3(a). In the temperature region below 150 K, the number of trapped electrons accumulated during cooling will be higher than that during heating (see point H in Fig. 4(b)). This will account for the reason why the PL intensity obtained on cooling below 150 K is lower than that obtained on heating (see Fig. 3(a)). If this scheme holds, the PL intensity of the thus cooled sample will be recovered to the initial value by

reheating the sample at temperatures above ~ 320 K. This is because, according to the scheme shown in Fig. 4(b), heating at temperatures above 320 K will reset the number of trapped electrons to zero, erasing the previous light irradiation history. As shown in Fig. 3(b), the recovery of the PL intensity was indeed observed after reheating the sample at 320 K, supporting the validity of our model.

In summary, we have shown that the induction heating with a graphite crucible under inert atmosphere is a simple but useful method to obtain highly UV luminescent g-SiO₂. The emission center responsible for the UV PL band is twofold-coordinated Si, showing the efficient $S_1 \rightarrow S_0$ luminescence band at 4.4 eV under excitation with ~ 5 -eV photons. The room-temperature internal and external quantum yields for the 4.4-eV PL band are 68% and 55%, respectively. We have also found that the 4.4-eV PL band shows irreversible temperature anti-quenching behaviors in the temperature region below ~ 320 K, indicating that the PL intensity is affected not only by temperature but also by light irradiation history. Thermally activated photoionization and the related charge trapping/detrapping events related to deep trap states are likely to be responsible for the irreversible anti-quenching phenomena.

¹F. L. Galeener, in *The Physics and Technology of Amorphous SiO₂*, edited by R. A. B. Devine (Plenum, New York, 1987), pp. 1–13.

²A. C. Wright and R. N. Sinclair, in *Structure and Imperfection in Amorphous and Crystalline Silicon Dioxide*, edited by R. A. B. Devine, J.-P. Duraud, and E. Dooryh e (Wiley, Chichester, 2000), pp. 121–150.

³Y. Tu, J. Tersoff, G. Grinstein, and D. Vanderbilt, *Phys. Rev. Lett.* **81**, 4899 (1998).

⁴L. Lichtenstein, M. Heyde, and H.-J. Freund, *Phys. Rev. Lett.* **109**, 106101 (2012).

⁵P. Y. Huang, S. Kurasch, J. S. Alden, A. Shekhawat, A. A. Alemi, P. L. McEuen, J. P. Sethna, U. Kaiser, and D. A. Muller, *Science* **342**, 224 (2013).

⁶L. C. Feldman, E. P. Gusev, and E. Garfunkel, in *Fundamental Aspects of Ultrathin Dielectrics on Si-based Devices*, edited by E. Garfunkel, E. Gusev, and A. Vul' (Kluwer Academic Publishers, Boston, 1998), pp. 1–24, and references therein.

⁷M. Yamane and Y. Asahara, *Glasses for Photonics* (Cambridge University Press, Cambridge, 2000).

⁸L. Tong, R. R. Gattass, J. B. Ashcom, S. He, J. Lou, M. Shen, I. Maxwell, and E. Mazur, *Nature* **426**, 816 (2003).

⁹R. A. Weeks, *J. Appl. Phys.* **27**, 1376 (1956).

¹⁰D. L. Griscom, *J. Non-Cryst. Solids* **73**, 51 (1985).

¹¹G. Pacchioni, in *Defects in SiO₂ and Related Dielectrics: Science and Technology*, edited by G. Pacchioni, L. Skuja, and D. L. Griscom (Kluwer, Dordrecht, 2000), pp. 161–195.

¹²A. H. Edwards, W. B. Fowler, and J. Robertson, in *Structure and Imperfection in Amorphous and Crystalline Silicon Dioxide*, edited by R. A. B. Devine, J.-P. Duraud, and E. Dooryh e (Wiley, Chichester, 2000), pp. 253–291.

¹³L. Skuja, A. N. Streletsky, and A. B. Pakovich, *Solid State Commun.* **50**, 1069 (1984).

¹⁴J. H. Stathis and M. A. Kastner, *Phys. Rev. B* **35**, 2972 (1987).

¹⁵H. Nishikawa, E. Watanabe, D. Ito, and Y. Ohki, *Phys. Rev. Lett.* **72**, 2101 (1994).

¹⁶L. Skuja, *J. Non-Cryst. Solids* **167**, 229 (1994).

¹⁷R. Boscaino, M. Cannas, F. M. Gelardi, and M. Leone, *Phys. Rev. B* **54**, 6194 (1996).

¹⁸M. Watanabe, S. Juodkakis, H.-B. Sun, S. Matsuo, and H. Misawa, *Phys. Rev. B* **60**, 9959 (1999).

¹⁹S. Agnello, R. Boscaino, M. Cannas, F. M. Gelardi, M. Leone, and B. Boizot, *Phys. Rev. B* **67**, 033202 (2003).

²⁰L. Skuja, *J. Non-Cryst. Solids* **239**, 16 (1998).

²¹V. A. Radzig, *J. Non-Cryst. Solids* **239**, 49 (1998).

²²A. N. Trukhin, *J. Non-Cryst. Solids* **357**, 1931 (2011).

²³D. L. Griscom, *J. Non-Cryst. Solids* **357**, 1945 (2011).

²⁴M. Itou, A. Fujiwara, and T. Uchino, *J. Phys. Chem. C* **113**, 20949 (2009).

- ²⁵S. Ikeda and T. Uchino, *J. Phys. Chem. C* **118**, 4346 (2014).
- ²⁶S. Sawai and T. Uchino, *J. Appl. Phys.* **112**, 103523 (2012).
- ²⁷F. L. Galeener and G. Lucovsky, *Phys. Rev. Lett.* **37**, 1474 (1976).
- ²⁸J. C. Mikkelsen, Jr. and F. L. Galeener, *J. Non-Cryst. Solids* **37**, 71 (1980).
- ²⁹S. K. Sharma, J. F. Mammone, and M. F. Nicol, *Nature* **292**, 140 (1981).
- ³⁰L. Skuja, *J. Non-Cryst. Solids* **149**, 77 (1992).
- ³¹I. Pelant and J. Valenta, *Luminescence Spectroscopy of Semiconductors* (Oxford University Press, Oxford, 2012), pp. 148–160.
- ³²Y. Zhao, C. Riemersma, F. Pietra, R. Koole, C. de M. Donegá, and A. Meijerink, *ACS Nano* **6**, 9058 (2012).
- ³³X. Ding, R. C. Dai, Z. Zhao, Z. P. Wang, Z. Q. Sun, Z. M. Zhang, and Z. J. Ding, *Chem. Phys. Lett.* **625**, 147 (2015).